Predictive Energy Management of a Power-Split Hybrid Electric Vehicle

H. Ali Borhan   Ardalan Vahidi   Anthony M. Phillips   Ming L. Kuang   Ilya V. Kolmanovsky

Abstract— *In this paper, a Model Predictive Control (MPC) strategy is developed for the first time to solve the optimal energy management problem of power-split hybrid electric vehicles. A power-split hybrid combines the advantages of series and parallel hybrids by utilizing two electric machines and a combustion engine. Because of its many modes of operation, modeling a power-split configuration is complex and devising a near-optimal power management strategy is quite challenging. To systematically improve the fuel economy of a power-split hybrid, we formulate the power management problem as a nonlinear optimization problem. The nonlinear powertrain model and the constraints are linearized at each sample time and a receding horizon linear MPC strategy is employed to determine the power split ratio based on the updated model. Simulation results over multiple driving cycles indicate better fuel economy over conventional strategies can be achieved. In addition the proposed algorithm is causal and has the potential for real-time implementation.*

I. INTRODUCTION

In Hybrid Electric Vehicles (HEVs) there are additional components, such as electric motors and batteries, which provide more flexibility to operate the powertrain system to meet the driver demand and minimize the fuel consumption. In other words, with respect to a conventional vehicle, there are more degrees of freedom for controls to satisfy driver demand. In general, the main components of HEVs may be classified into an energy source (fuel), energy convertors (engine, generators, and motors) and an energy accumulator (battery or ultracapacitor). Torque couplers or/and speed couplers may be employed as a link between these components [1]. Different hybrid configurations such as series, parallel, and power-split have been developed depending on the arrangement of these components. Power-Split or Parallel-Series types which provide both series and parallel functionality have been the preferred configuration by many auto-makers. The Ford Escape hybrid and Toyota Prius both use a power-split configuration.

H. Borhan (corresponding author) is a PhD student of mechanical engineering at Clemson University, Clemson, SC 29634 E-mail: hborhan@clemson.edu.

A. Vahidi is an Assistant Professor of Mechanical Engineering at Clemson University, Clemson, SC 29634 E-mail: avahidi@clemson.edu.

A. M. Phillips is a Senior Technical Leader at Ford Research and Advanced Engineering, Ford Motor Company, Dearborn, MI 48124, E-mail: aphilli8@ford.com.

M. L. Kuang is a Technical Leader with Ford Research and Advanced Engineering, Ford Motor Company, Dearborn, MI 48124, E-mail: mkuang@ford.com.

I.V. Kolmanovsky is a Technical Leader at Ford Research and Advanced Engineering, Ford Motor Company, Dearborn, MI 48124, E-mail: ikolmano@ford.com.
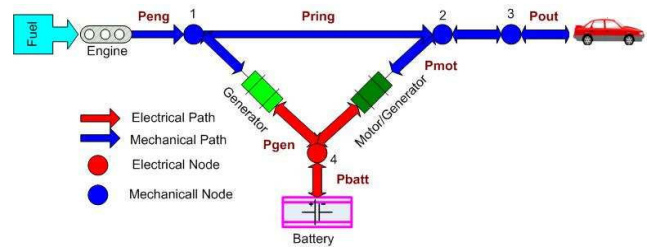
Fig. 1. Power flow of a power-split HEV

Figure 1 schematically shows the power flow in the mechanical and electrical paths in a power split hybrid. The electrical and mechanical nodes represent the components which combine power flows. In this configuration, the engine and the generator are connected to the planet carrier and sun gear of a planetary gear set (speed coupler at mechanical Node 1) respectively. The output of the planetary gear set is coupled with another motor/generator electric machine through a torque coupler (mechanical Node 2) and powers the vehicle driveline. In this configuration, because the generator can also work in a motoring mode and deliver energy to the speed coupler, circulation of power around the triangular loop of the diagram can be utilized to shift the engine's operating point to a more efficient region. Also the battery provides another degree of freedom by its energy buffering capability. Thus, there are two degrees of freedom for energy management of these HEVs . These two degrees of freedom and the many modes of operation of a power-split hybrid increase the flexibility for running the vehicle more efficiently, while at the same time the complex configuration renders design of the energy management strategy quite challenging.

The need for systematic design of a near-optimal energy management strategy is addressed in this paper by a Model Predictive Control (MPC) approach [2]. The energy management problem is formulated as an optimization problem over a future time window during which the objective is to i) minimize fuel use, ii) reduce service brake use, and iii) prevent over-charge and -discharge of the battery while respecting kinematic equality constraints and several time-varying inequality constraints of the engine, motor, generator, and the battery. The solution of this nonlinear optimization determines the "optimal" distribution of power demand between the engine, motor, generator, and service brakes.

An analytical solution to such a nonlinear constrained

optimization problem does not exist in general. Therefore in the past researchers have proposed numerical solutions, e.g. by using dynamic programming (DP) or have simplified the dynamic optimization problem to an equivalent instantaneous optimization in a family of ECMS (Equivalent Consumption Minimization Strategy) schemes. A more detailed review of these optimal control methods along with heuristic rule-based methods can be found in [3] and [4]. Most of the existing literature has focused on the less complicated parallel and series configurations and only a few papers address the case for power-split hybrids. One of those is [5] where both DP and ECMS were applied and compared for the Toyota Prius power-split HEV.

Obtaining the optimal solution using DP requires knowledge of future driving cycle and therefore is non-causal. Together with high computational demand of DP, this prevents its real-time implementation. The ECMS methods, on the other hand, are less intensive in computations and causal but may be short-sighted and are sensitive to their tuning parameters. The MPC design proposed in this paper overcomes some of these shortcomings. In the MPC approach, the optimization is solved over a future prediction horizon (therefore less-likely to make short-sighted decisions). At the same time knowledge of the future drive cycle is not assumed. Instead a model is used to project the torque demand and the resulting velocity over a future prediction horizon (therefore causal). To prevent the computational cost of a nonlinear optimization problem, the nonlinear plant model and the constraints are linearized at each sample time; this reduces the nonlinear optimization problem to a quadratic program for which efficient real-time solutions exist [6]. Moreover, the relation between MPC tuning parameters and the results may be more transparent and systematic than that of ECMS methods.

Because MPC is a model-based control method, the vehicle model is first derived and the constraints are specified in Section II. The optimization problem and the linear MPC design are laid out in Section III. Simulation results in three different driving scenarios are presented in Section IV followed by the Conclusions.

II. THE PLANT MODEL

A schematic of a power-split HEV configuration is shown in Figure 2. What makes this configuration different from the series and parallel configurations is the split of engine power by a speed coupler (planetary gear set) which allows both series and parallel power flow modes. Because the focus of the paper is a model-based optimization method, a model of the system is derived in this section. For more details, the reader is referred to the literature [7], [5].

In general, the system dynamics can be divided into powertrain dynamics and battery dynamics. The following assumptions are made:

- Dynamics of engine, motor and generator are fast with respect to the dynamics of powertrain and vehicle.
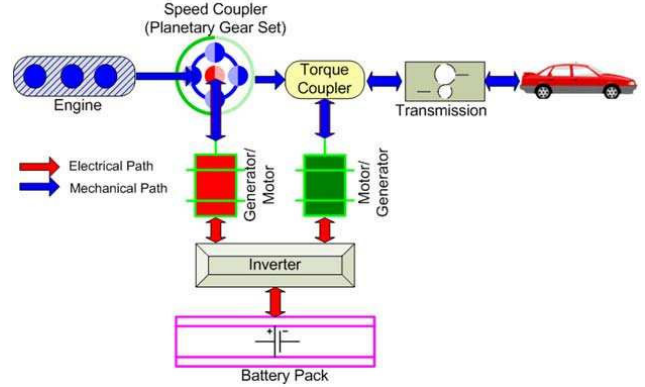

Fig. 2. A Power-Split HEV Configuration

- The motor is directly connected to the ring gear of the speed coupler.
- The power loss in the final transmission can be ignored with respect to other sources of power losses.
- All components connecting motor to wheel are rigid

Consequently, the powertrain dynamics are summarized as:

$$J_{gen}\frac{d\omega_{gen}}{dt} = \tau_{gen} + F \times N_S$$
$$J_{eng}\frac{d\omega_{eng}}{dt} = \tau_{eng} - F \times (N_S + N_R)$$
$$J_{mot}\frac{d\omega_{mot}}{dt} = \tau_{mot} - \frac{\tau_{drive} + \tau_{brake}}{g_f} + F \times N_R \quad (1)$$
$$m\frac{dV}{dt} = \frac{\tau_{drive}}{r_w} - \frac{1}{2}\rho A_f C_d V^2 - mg\sin(\theta) - \mu mg\cos(\theta)$$

Where J_{eng}, J_{gen}, J_{mot} are the inertia of the engine, generator and motor, N_S, N_R are the radius of the sun and ring gears, τ_{eng}, τ_{gen}, τ_{mot} are the engine, generator and motor torques, ω_{eng}, ω_{gen}, ω_{mot} are the engine, generator and motor speeds, τ_{drive} is the drive shaft torque , τ_{brake} is the friction or service brake torque, V, m, A_f are the speed, mass and frontal area of the vehicle, r_w is the wheel radius, μ is the friction coefficient, C_D and ρ are the drag coefficient and air density, g_f is the final gear ratio, θ is the road grade and g is gravitational acceleration. Also F is the interaction force between different parts of the power-train. For example, $F \times N_S$ is the reaction torque on the sun gear. Also there are two kinematic equality constraints between velocities:

$$N_s\omega_{gen} + N_R\omega_{mot} = (N_s + N_R)\omega_{eng} \quad (2)$$

and

$$\omega_{mot} = \frac{g_f}{r_w}V \quad (3)$$

Substituting equations (2)-(3) into the dynamics of the powertrain and eliminating the interaction force F, between them, the powertrain dynamics are reduced to,

$$\begin{bmatrix} J_{eng} + \left(\frac{N_S+N_R}{N_S}\right)^2 J_{gen} & -\left(\frac{N_R(N_S+N_R)}{N_S^2}\right)J_{gen} \\ -\left(\frac{N_R(N_S+N_R)}{N_S^2}\right)J_{gen} & J_{mot} + \left(\frac{N_R}{N_S}\right)^2 J_{gen} + \frac{mr_w^2}{g_f^2} \end{bmatrix} \begin{bmatrix} \frac{d\omega_{eng}}{dt} \\ \frac{d\omega_{mot}}{dt} \end{bmatrix}$$

$$= \begin{bmatrix} 1 & 0 & \left(\frac{N_S+N_R}{N_S}\right) & 0 \\ 0 & 1 & -\left(\frac{N_R}{N_S}\right) & -\frac{1}{g_f} \end{bmatrix} \begin{bmatrix} \tau_{eng} \\ \tau_{mot} \\ \tau_{gen} \\ \tau_{brake} \end{bmatrix} + \begin{bmatrix} 0 \\ -\frac{1}{g_f} \end{bmatrix} \tau_{resist}$$

$$(4)$$

where the resistance torque is defined by,

$$\tau_{resist} = r_w mg \left(\mu\cos\theta + \sin\theta\right) + \frac{1}{2}\rho C_d A_f r_w^3 \left(\frac{\omega_{mot}}{g_f}\right)^2 \quad (5)$$

The battery state of charge (SOC) is an important variable in energy management of HEVs. Its dynamics are described by [1],

$$\frac{dSOC}{dt} = -\frac{V_{oc} - \sqrt{V_{oc}^2 - 4(P_{batt})R_{batt}}}{2C_{batt}R_{batt}} \quad (6)$$

where V_{oc}, R_{batt}, C_{batt} are the battery's open-circuit voltage, internal resistance and capacity respectively and $P_{batt} = P_{mot} + P_{gen} + P_{motor}^{loss} + P_{gen}^{loss}$ represents the charging and discharging power of the battery and includes motor and generator losses. In our model, positive power indicates battery discharging and negative power indicates charging. To model the motor/generator power losses, a surface is fitted to experimental data. An experimental map of the engine relates the fuel consumption rate to engine speed and engine torque. The Willan's line method is used to approximate this map resulting in a closed-form formula,

$$\dot{m}_f = \frac{aT_{eng}\omega_{eng} + b\omega_{eng} + c\omega_{eng}^3}{\bar{a} + \bar{b}\omega_{eng} + \bar{c}\omega_{eng}^2} \quad (7)$$

where $\dot{m}_f$ is the fuel consumption rate and a, b, c, $\bar{a}$, $\bar{b}$, and $\bar{c}$ are constant parameters.

Finally, several physical constraints of the model are summarized as:

$$SOC^{\min} \leq SOC \leq SOC^{\max}$$
$$0 \leq \omega_{eng} \leq \omega_{eng}^{\max}$$
$$\omega_{mot}^{\min} \leq \omega_{mot} \leq \omega_{mot}^{\max}$$
$$\omega_{gen}^{\min} \leq \omega_{gen} \leq \omega_{gen}^{\max}$$
$$0 \leq \tau_{eng} \leq \tau_{eng}^{\max}$$
$$\tau_{mot}^{\min} \leq \tau_{mot} \leq \tau_{mot}^{\max}$$
$$\tau_{gen}^{\min} \leq \tau_{gen} \leq \tau_{gen}^{\max}$$
$$0 \leq \tau_{brake}$$
$$P_{batt} \leq V_{oc}^2 / 4R_{batt}$$

where $*^{\min}$ and $*^{\max}$ represent the minimum and maximum bounds on the parameters. These bounds on τ_{eng}, τ_{gen}, and τ_{mot} are variables and are functions of engine, generator and motor speeds respectively.

III. CONTROL SYSTEM STRUCTURE

The power management module of a power-split HEV determines the engine, generator, motor, and service brake torques based on the driver's demanded torque and loads from the road and auxiliary subsystems. Because of the dynamic nature of the power demand, this is a dynamic decision making problem. Its objective is to minimize fuel consumption while ensuring all the constraints are enforced pointwise-in-time. In this work, we manage the complexity of this problem by breaking it into two levels. The first or supervisory level finds the optimum values for the two independent degrees of freedom of the system (here engine speed and engine torque) at each sample time. These optimum values are issued as references to the second or low-level controller. The low-level controller determines the engine, motor, generator, and brake torques required to follow the references set by the supervisory layer. A block-diagram schematic is shown in Figure 2. The low-level controller can use standard control loops for reference tracking. In what follows, the focus is on the supervisory control design.
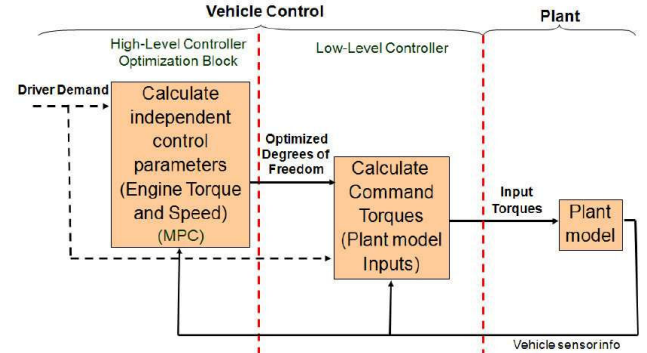

Fig. 3. Structure of the Control System

At the supervisory level, the power management problem can be viewed as a constrained nonlinear dynamic optimization problem. The need for real-time implementable optimization-based approach has motivated us to use a Model Predictive Control (MPC) formulation. In short, MPC contains three steps: First, based on an internal (usually reduced-order) model of the plant, it predicts the plant outputs along a future time horizon. Then it calculates a future control sequence that minimizes a performance index which reflects the optimization goals subject to the constraints. Finally it applies just the first of this control sequence to the plant. The process is repeated at the next time step by moving the prediction horizon one step forward.

A. Nonlinear Internal Model

In the MPC's internal prediction model, we ignore the powertrain inertial losses in comparison to other slower dynamics. This reduces the model complexity and increases computational efficiency. Also because the speed of the vehicle is controlled by the driver, the vehicle speed dynamics

are moved outside of the internal model. The remaining dynamic state of this internal model is the battery's state of charge. As briefly noted earlier, the model is driven by 3 independent inputs. The service brake torque is always an independent input and therefore a fixed degree of freedom. There are several other choices for the other degrees of freedom. In this work, we have chosen the engine speed and engine torque as the other two degrees of freedom. These are the free optimization variables in the supervisory control formulation and are chosen to minimize the following finite-horizon cost function at each sample time:

$$\min_{\vec{u}(t)} J = \int \left\| \vec{L}(x;\vec{u},\vec{v}) \right\|^2 dt \qquad (8)$$

subject to

$$\begin{cases} \dot{x} = f(x;\vec{u},\vec{v}) & x^{min} \le x \le x^{max} \\ \vec{y}_r = \vec{g}(x;\vec{u},\vec{v}) & \vec{y}_c^{min} \le \vec{y}_c \le \vec{y}_c^{max} \\ \vec{y}_c = \vec{g}(x;\vec{u},\vec{v}) & \vec{u}^{min} \le \vec{u} \le \vec{u}^{max} \end{cases} \qquad (9)$$

where

$$x = [SOC], \quad \vec{u} = \begin{bmatrix} \tau_{eng} \\ \omega_{eng} \\ \tau_{brake} \end{bmatrix}, \quad \vec{v} = \begin{bmatrix} \tau_{drive} \\ V \end{bmatrix}$$

$$\vec{y}_r = \begin{bmatrix} SOC \\ \dot{m}_f \end{bmatrix}, \quad \vec{y}_c = \begin{bmatrix} P_{batt} \\ \omega_{gen} \\ \tau_{mot} \\ \tau_{gen} \end{bmatrix}$$

are the vectors of state, control inputs, measured inputs, tracking outputs and constrained outputs respectively. Due to practical limits, the SOC should be kept around a desired value (SOC_r). Therefore the performance index penalizes deviations in state of charge in addition to fuel rate and brake use. The integrand in equation (8) is defined as,

$$\vec{L}(x;\vec{u},\vec{v}) = \begin{bmatrix} w_{SOC}(SOC - SOC_r), & w_f \dot{m}_f, & w_b \tau_{brake} \end{bmatrix}^T$$

where w_{SOC}, w_f and w_b are penalty weights.

B. Standard Linear MPC

Because the MPC control strategy at the supervisory level is based on the standard MPC for linear systems, it is briefly explained in this section. More details can be found in [2], [8]. A finite-horizon quadratic cost function penalizes deviation of the system outputs y from the corresponding references r. In its more general form, it can be formulated as:

$$\min_{\Delta U} J = \sum_{i=0}^{P-1} \|u(k+i|k) - u_{target}(k)\|_{w_i^u}^2 +$$

$$\|\Delta u(k+i|k)\|_{w_i^{\Delta u}}^2 + \|y(k+i+1|k) - r(k+i+1)\|_{w_{i+1}^y}^2 + \rho_\varepsilon \varepsilon^2 \qquad (10)$$

subject to

$$\begin{cases} x(k+1) = Ax(k) + B_u u(k) + B_v v(k) \\ y(k) = Cx(k) + D_v v(k) \end{cases}$$

$$u_i^{min} \le u(k+i|k) \le u_i^{max}$$

$$\Delta u_i^{min} \le \Delta u(k+i|k) \le \Delta u_i^{max}$$

$$-\varepsilon + y_i^{min} \le y(k+i+1|k) \le y_i^{max} + \varepsilon$$

$$\Delta u(k+i|k) = 0; j = M, ..., P$$

$$\varepsilon \ge 0$$

where P is the prediction horizon, M is the control horizon, $\Delta U = [\Delta u(k|k), ..., \Delta u(k+M-1|k)]^T$ is the sequence of input increments to be optimized, w_i^u, $w_i^{\Delta u}$, w_{i+1}^y are the weighting factors at the ith sample time, $x(k) \in R^n$ is the state vector, $u(k) \in R^m$ is the vector of manipulated variables, $y(k)$ is the vector of outputs and ε is the softening variable. Using the discrete model of the system, the outputs over a future prediction horizon are predicted by:

$$y(k+i+1|k) = C[A^{i+1}x(k) +$$

$$\sum_{l=0}^{i} A^i B_u \left(u(k-1) + \sum_{j=0}^{l} \Delta u(k+j|k) \right) + \qquad (11)$$

$$B_v v(k+l|k)] + D_v v(k)$$

Substituting predicted trajectories of outputs into the performance index J, the optimization problem can be formulated as a Quadratic Program (QP),

$$\left[\Delta U^{opt}, \varepsilon \right] = \arg\min_{\Delta U, \varepsilon} \frac{1}{2} \Delta U^T H \Delta U + F^T \Delta U \qquad (12)$$

subject to

$$G_u \Delta U + G_\varepsilon \varepsilon \le W + Sx(k)$$

where $H, F, G_u, G_\varepsilon, W$, and S are constant matrices and functions of references, measured inputs, input targets, the last control input, and the measured or estimated states at the current sample time [2], [8]. After solving this standard QP problem and obtaining the optimal input sequences ΔU^{opt}, the control input to the plant is obtained by

$$u(k) = u(k-1) + \Delta u^{opt}(k|k) \qquad (13)$$

C. The MPC-Based Control Strategy

The nonlinear model is linearized at each sample time around its current operating point and the control input is generated by applying MPC on this updated linear model of the system. The MPC problem is formulated as a QP problem with a linear model and linear constraints to be solved at each sample time. The stability and disturbance rejection properties for this approach are addressed in the literature [9], [10]. At each step k the following steps are taken:

1- Measurment/estimation of system state ($SOC(k)$)

2- Prediction of the torque demand and vehicle speed (measured inputs) over the next prediction horizon:

The future driver torque demand, which is unknown, is assumed to be exponentially decreasing over the prediction horizon, i.e.

$$\tau_{drive}((k+i)T) = \tau_{drive}(kT)e^{\left(\frac{-iT}{T_d}\right)} \qquad i = 1,\ 2,\ \cdots,\ P \tag{14}$$

where $\tau_{drive}(kT)$ is the known value of the torque demand at the beginning of the prediction horizon and T_d determines the decay rate. Due to frequent variation of torque demand in a driving cycle, assumption of a decaying torque demand was found to be more reasonable than a constant-torque assumption (which is the MPC default for measured disturbances). This was later confirmed by the simulation results.

By using the above torque model and by numerical integration of the vehicle longitudinal dynamics over the future horizon, the future velocity profile is predicted,

$$V((k+i)T) = V(kT) + \frac{1}{m}\int_{kT}^{(k+i)T} \tau_{drive}(t)e^{\left(\frac{-t}{T_d}\right)} \\ -\frac{1}{2}\rho C_D A_f V(t)^2 - mg\cos(\theta(t)) + \mu mg\sin(\theta(t))dt \tag{15}$$

where $V(kT)$ is the actual value of the velocity at the beginning of the prediction horizon. Here we assign $\theta = 0$ in the prediction model if grade information is not available.

3- Linearization of the nonlinear internal model around an operating point and update of linear system matrices:

$$\begin{cases} \dot{x} = \tilde{A}x + \tilde{B}_u u + \tilde{B}_v v + \tilde{F} \\ y = \tilde{C}x + \tilde{D}_u u + \tilde{D}_v v + \tilde{G} \end{cases} \tag{16}$$

where

$$\begin{aligned} \tilde{A} &= \left(\frac{\partial f}{\partial x}\right)_{(x_0,u_0,v_0)} ; \tilde{B}_u = \left(\frac{\partial f}{\partial u}\right)_{(x_0,u_0,v_0)} \\ \tilde{B}_v &= \left(\frac{\partial f}{\partial v}\right)_{(x_0,u_0,v_0)} ; \tilde{C} = \left(\frac{\partial [g_r,g_c]}{\partial x}\right)_{(x_0,u_0,v_0)} \\ \tilde{D}_u &= \left(\frac{\partial [g_r,g_c]}{\partial u}\right)_{(x_0,u_0,v_0)} ; \tilde{D}_v = \left(\frac{\partial [g_r,g_c]}{\partial v}\right)_{(x_0,u_0,v_0)} \\ \tilde{F} &= f(x_0,u_0,v_0) - \tilde{A}x_0 - \tilde{B}_u u_0 - \tilde{B}_v v_0 \\ \tilde{G} &= g(x_0,u_0,v_0) - \tilde{C}x_0 - \tilde{D}_u u_0 - \tilde{D}_v v_0 \end{aligned} \tag{17}$$

To remove direct injection of the inputs in the output equations in accordance to standard MPC formulation (section 2), the linearized system is augmented with fast filters with time constant of T_f ,

$$\begin{bmatrix} \dot{x} \\ \dot{x}_a \end{bmatrix} = \underbrace{\begin{bmatrix} [0]_{1\times 1} & \tilde{B}_u \\ [0]_{3\times 1} & -1/T_f [I]_{3\times 3} \end{bmatrix}}_{A^c} \begin{bmatrix} x \\ x_a \end{bmatrix} + \\ \underbrace{\begin{bmatrix} [0]_{1\times 3} \\ 1/T_f [I]_{3\times 3} \end{bmatrix}}_{B_u^c} \vec{u} + \underbrace{\begin{bmatrix} \tilde{B}_v & [1]_{1\times 1} & [0]_{1\times 6} \\ [0]_{3\times 2} & [0]_{3\times 1} & [0]_{3\times 6} \end{bmatrix}}_{B_v^c} \begin{bmatrix} \vec{v} \\ \tilde{F} \\ \tilde{G} \end{bmatrix} \\ [y] = \underbrace{\begin{bmatrix} \tilde{C} & \tilde{D}_u \end{bmatrix}}_{C^c} \begin{bmatrix} x \\ x_a \end{bmatrix} + \underbrace{\begin{bmatrix} \tilde{D}_v & [0]_{6\times 1} & [I]_{6\times 6} \end{bmatrix}}_{D_v^c} \begin{bmatrix} \vec{v} \\ \tilde{F} \\ \tilde{G} \end{bmatrix} \tag{18}$$

4- Discretization of the augmented linear system matrices $(A^C,\ B_u^C,\ B_v^C,\ C^C,\ D_v^C)$ in order to evaluate discretized linear system matrices $A,\ B_u,\ B_v,\ C,\ D_v$.

5- Application of standard linear MPC explained in the previous section to the updated model to find control inputs for next sample time.

6- Repetition of the previous steps at the next sample time.

IV. SIMULATION RESULTS AND DISCUSSION

A. MPC Controller Tuning

In standard MPC, the adjustable parameters are penalty weights and prediction and control horizons. In addition in this work, the time constant T_d in the torque model (14) is another tuning parameter. In all simulations, the sample interval of MPC is fixed to 1 second. Also, the prediction and control horizons are fixed to 5. Via various simulations and observations we found that the results can be improved if the penalty weights and the time constant T_d are varied with the level of torque demand. The following rules for selecting the weights and the time constant were established:

if $\tau_{drive}(kT) \geq 1000$
    $W_{SOC} = 1, W_{\dot{m}_f} = 1$ and $T_d = 0.1$
elseif $450 \leq \tau_{drive}(kT) < 1000$
    $W_{SOC} = 1, W_{\dot{m}_f} = 1$ and $T_d = 1$
elseif $100 \leq \tau_{drive}(kT) < 450$
    $W_{SOC} = 1, W_{\dot{m}_f} = 10$ and $T_d = 1$
elseif $0 \leq \tau_{drive}(kT) < 100$
    $W_{SOC} = 1, W_{\dot{m}_f} = 50$ and $T_d = 10$
elseif $\tau_{drive}(kT) < 0$
    $W_{SOC} = 0, W_{\dot{m}_f} = 1e6$ and $T_d = 0.1$

Here a smaller T_d (faster decay) is chosen for larger driver torque demands. This is motivated by the observation that periods of large torque demand are very short in a typical driving cycle. In other words, a large torque demand is not expected to prolong much. A number of trial and error revealed that choice of a larger penalty on fuel rate during periods of low torque demand improved the MPC

performance. One possible explanation is that the engine is less efficient at low torque levels and its use should be further penalized. Finally when the torque demand is negative, the weight on SOC is set to zero to encourage regeneration into the battery even if that requires deviation from the desired state of charge. At the same time the fuel consumption is penalized with a very large weight to discourage use of the engine. Except for the braking mode, the brake torque is penalized by a large weight of 1000. The reference values are taken to be constant and equal to 0.65 and 0 for state of the charge and fuel rate respectively.

B. Acceleration-Cruise-Braking Scenario

In order to analyze the performance of the developed control system for energy management of a power-split HEV, we used different driving scenarios. The first simulated driving scenario includes a 0 to 70 (km/hr) acceleration, then a constant 70 (km/h) cruise, and finally decelerating to a stop. This scenario covers acceleration, deceleration, and cruise. The simulation results are presented in figures 4-6.
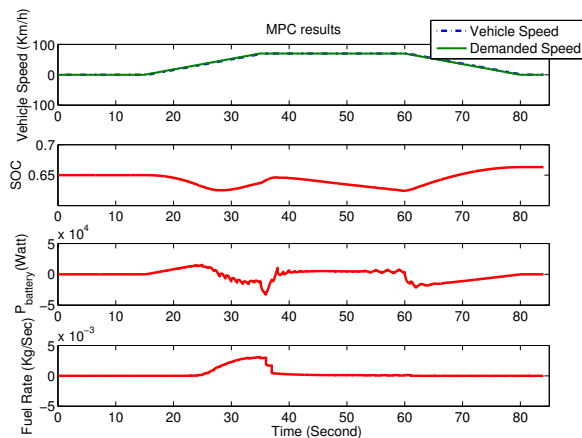

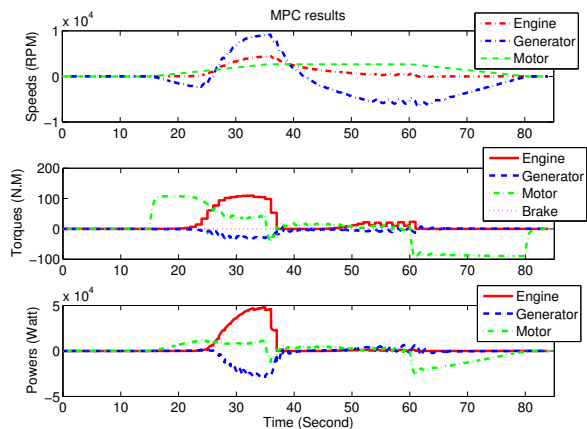Fig. 4. MPC results: Vehicle speed, SOC, battery power, and fuel rate

Fig. 5. MPC results: Engine, motor, and generator's speed, torque, and power
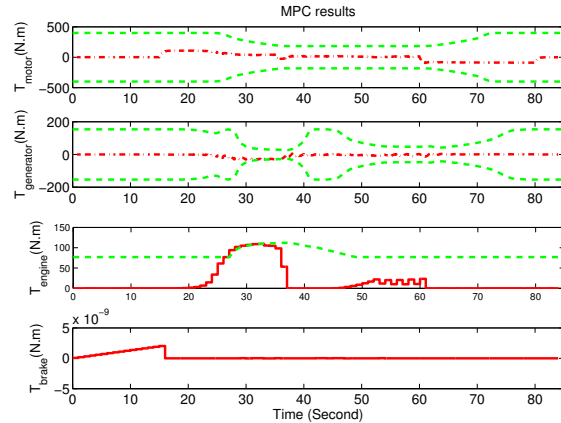

Fig. 6. MPC results: Engine, motor, and generator's torque and constraints

We observe from these results that during acceleration (15 to 35 seconds), the motor assists the engine to deliver the required power and the SOC decreases. The generator provides negative or reaction torque that increases transmission of engine torque to the wheels. This operation is called *positive-split*. Later during the cruise mode (35 to 60 seconds), the controller decreases the generator speed to negative values and the generator works in the motoring mode. During this mode, the vehicle speed is relatively high and the power demand is low which causes the generator speed to decrease to negative values and reduces the engine speed according to equations (2)-(3). In other words, a part of the engine power is re-circulated through the motor and generator to decrease engine rotational speed while it delivers the demanded power. This mode is called *negative-split*. Eventually during deceleration, the motor works in the generating mode and energy is recuperated into the battery and the battery state of the charge is increased. This mode is the *regenerative braking* mode. As shown, MPC can perform well in all operating modes. In addition as shown in figure 6, the controller enforces all the variable constraints on the engine, motor, and generator torques.

C. Simulation results with standard driving cycles

In order to analyze the performance of the developed control system with respect to fuel economy, two different standard driving cycles were tested. Figures 7-8 show simulation results over UDDS (Urban Dynamometer Driving Schedule also called FTP 72) cycle. The controller satisfies all the constraints and maintains the SOC near the desired value of 0.65. For the given driving cycle, the simulation yields an equivalent fuel economy equal to 74.93 mile per gallon (mpg). The PSAT 6.2 simulation program developed by Argonne National Laboratory (ANL) [11] which uses a rule-based power management strategy calculates a comparable equivalent fuel economy of 71.56 (mpg) for the same cycle.

The MPC performance is also tested in a highway driving scenario, the HWFET (Highway Fuel Economy Driving
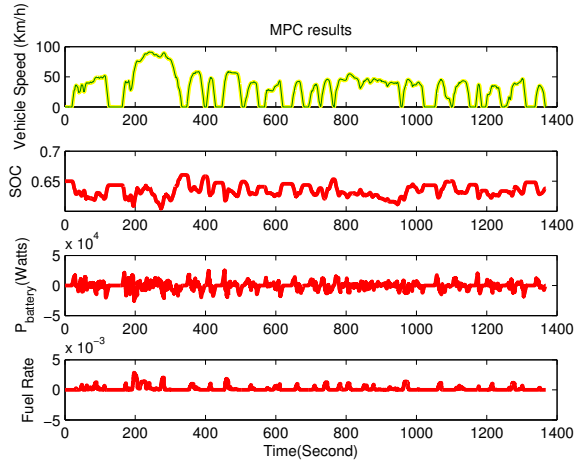
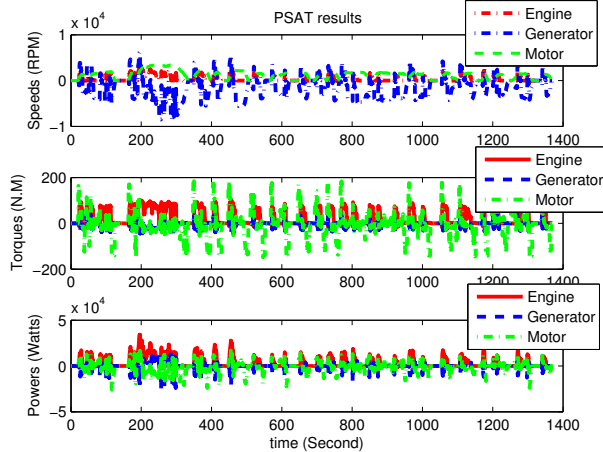Fig. 7. Vehicle speed, SOC, battery power, and fuel rate

Fig. 8. Engine, motor, and generator speeds, torques, and powers

Schedule also called FHDS) cycle. For this driving cycle, MPC yields equivalent fuel economy equal to 67.76 (mpg) with final SOC=0.69. With the same driving cycle, the PSAT software calculates a comparable equivalent fuel economy equal of 66.42 (mpg). These simulation results are promising and encourage stepping toward experimental validation which is the plan for future work.

V. CONCLUSIONS

In the existing literature, optimal power management of HEVs has relied mostly on dynamic programming (DP) or minimization of an instantaneous cost function in a family of ECMS approaches. The drawbacks to DP are its cycle-dependence and computational intensity. The ECMS may be short-sighted and also very sensitive to its tuning parameters. The MPC formulation presented in this paper has the advantages of being i) predictive in nature ii) adaptive to changes in the plant operating point and external disturbances, and iii) systematic to tune with less parameter-sensitivity. It achieves very good fuel economy via on-line optimization, while, at the same time, it is causal and

therefore potentially real-time implementable. The power-split hybrid which was the subject of this work, is one of the most complex types of HEVs having strong non-linearities, kinematic equality constraints, and time-varying inequality constraints. This complexity was reflected in the high-fidelity model that was used. We demonstrated that by constantly linearizing and updating the prediction model and the constraints, a linear MPC makes decisions that qualitatively match those of a well-tuned conventional power management strategy. Also quantitatively, the fuel economies achieved with MPC are better than those re-ported by the rule-based PSAT simulation software. Further simulation and experimental investigation are required to validate these quantitative results.

VI. ACKNOWLEDGEMENTS

REFERENCES

[1] S. E. Gay A. Emadi M. Ehsani, Y. Gao, *Modern Electric, Hybrid Electric, and Fuel Cell Vehicles: Fundamentals, Theory, and Design*, CRC, 2004.
[2] J. M. Maciejowski, *Predictive Control with Constraints*, Prentice Hall, 2002.
[3] A. Sciarretta and L. Guzzella, "Control of hybrid electric vehicles," *IEEE Control Systems Magazine*, vol. 27, no. 2, pp. 60–70, 2007.
[4] P. Pisu and G. Rizzoni, "A comparative study of supervisory control strategies for hybrid electric vehicles," *IEEE Transactions on Control Systems Technology*, vol. 15, no. 3, pp. 506–518, 2007.
[5] J. Liu and H. Peng, "Modeling and control of a power-split hybrid vehicle," *IEEE Transactions on Control Systems Technology*, vol. accepted for inclusion in a future issue of this journal, 2008.
[6] A. Bemporad, "Model predictive control design: New trends and tools," in *Proceedings of the IEEE Conference on Decision and Control*, 2006, pp. 6678–6683.
[7] J. Czubay F. U. Syed, M. L. Kuang and H. Ying, "Derivation and experimental validation of a power-split hybrid electric vehicle model," *IEEE Transactions on Control Systems Technology*, vol. 54, no. 6, pp. 1731–1747, 2006.
[8] M. M. Seron G. C. Goodwin and J. A. Dona, *Constrained Control and Estimation*, Springer, 2005.
[9] S. Oliveira, *Model Predictive Control for Constrained Nonlinear Systems*, vdf Hochschulverlag AG, 1996.
[10] J. H. Lee and N. l. Ricker, "Extended Kalman filter based nonlinear model predictive control," *Industrial Engineering and Chemical Research*, vol. 33, no. 6, pp. 1530–1541, 1994.
[11] Argonne National Laboratory, "Powertrain System Analysis Toolkit," commercial software.